Chapter 5

Rheological measurements with rough walls over a porous medium

5.1 Motivation

As mentioned in Chapter 2, the rheometer was designed to reduce the effect of secondary flows. This was achieved by increasing the ratio between height and shearing gap, rotating the outer cylinder, fixing the top and bottom boundaries, and also by making the torque measurements in the middle section (away from the top and bottom boundaries, where the secondary flows are present). While this design might help to reduce the effect of secondary flows, it limits the study of settling particles with low loading fraction. When the loading fraction is less than 20% and the particles are denser than the suspending liquid, the height of the settled particles's column is less than the height of the test cylinder. Therefore the particles may not reach the measurement zone until the shear rate is high enough to fluidize them (see Chapter 6 for particle resuspension analysis). To study the rheology of low loading fractions, the experimental setup was modified by adding a layer of glass beads at the bottom of the rheometer. These glass beads form a porous medium at the lower part of the rheometer, approximately 2 cm below the test cylinder. The polystyrene particles are placed over the glass beads, guaranteeing the presence of particles in the middle section for all the loading fractions tested. This enables the study of loading fractions of 10 and 20% at low shear rates. The presence of a porous medium also adds roughness to the lower boundary , which can affect the behavior of the suspending liquid.

5.2 Modification of the experiment and porous medium configuration

The porous medium was formed using spherical glass beads with a density of 2520 (kg/m^3) and 4 (mm) in diameter size. Glass beads (2.36 l) were poured into the rheometer and filled the bottom

region. Once the glass beads were poured and evenly distributed along the rheometer annulus, they were sheared at different speeds to account for any change of particle packing. To avoid excessive shearing of the porous medium, the walls at the bottom of the rheometer were left smooth. The height of the glass beads layer was then measured with the help of a vernier to determine the packing of the porous medium. These measurements were made dry and it is assumed that the effect of water on the packing of glass beads is negligible due to the high density of the glass beads. The glass beads packing was calculated as 0.63. Koos (2009) measured the random close packing (RCP) of spherical glass beads of 3 mm diameter with the same density and found that RCP=0.626. Using the fit found by Zou and Yu (1996) and considering the model of O'Hern et al. (2002) to calculate the random close packing of 4 mm glass beads, a value of 0.637 is obtained, which is very close to the one calculated based on the glass beads height measurements.

The volume of glass beads ensures that the maximum height reached by the porous medium after being sheared is no higher than the bottom cylinder height. Based on the glass beads height measurements, the porous medium is 1.9 cm below the test cylinder. After shearing the glass beads a change in the shape of the top surface is observed. The glass beads move slightly towards the inner cylinder, forming an angle where the porous height is slightly shorter next to the outer wall. After this re-arrangement of the glass beads, the porous medium is still approximately 1.9 cm in average below the test section. Because this re-accommodation of the beads did not seem to change the average height of the porous medium, the packing of the glass beads is considered to remain the same. If further dilatancy were to occur during the run of an experiment, and the porous medium packing went from close to loose, the maximum height reached by the particles would be 1.3 cm below the test cylinder (this is based on the random loose packing measured by Koos (2009)). Thus the glass beads do not reach the middle section. A scheme of the modified experimental setup is shown in Figure 5.1.

Once the porous medium was prepared, polystyrene particles were poured on top. For these experiments the total volume considered when calculating the loading fraction does not include the volume occupied by the glass beads. With this configuration the volume of particles needed to obtain a loading fraction of 10% is lower than for the case without a porous medium.

5.3 Torque measurements of polystyrene particles over a porous medium with $\rho_p/\rho = 1.05$

Figure 5.2 shows the torque measurements as a function of shear rate for $\bar{\phi} = 10\%$. For shear rates lower than 60 s^{-1}, the torque shows a linear dependance on the shear rate. There appears to be a change in the torque dependance for shear rates higher than 60 s^{-1}. The torque increases more rapidly and its dependance on shear rate is no longer linear. The torques for these higher shear rates

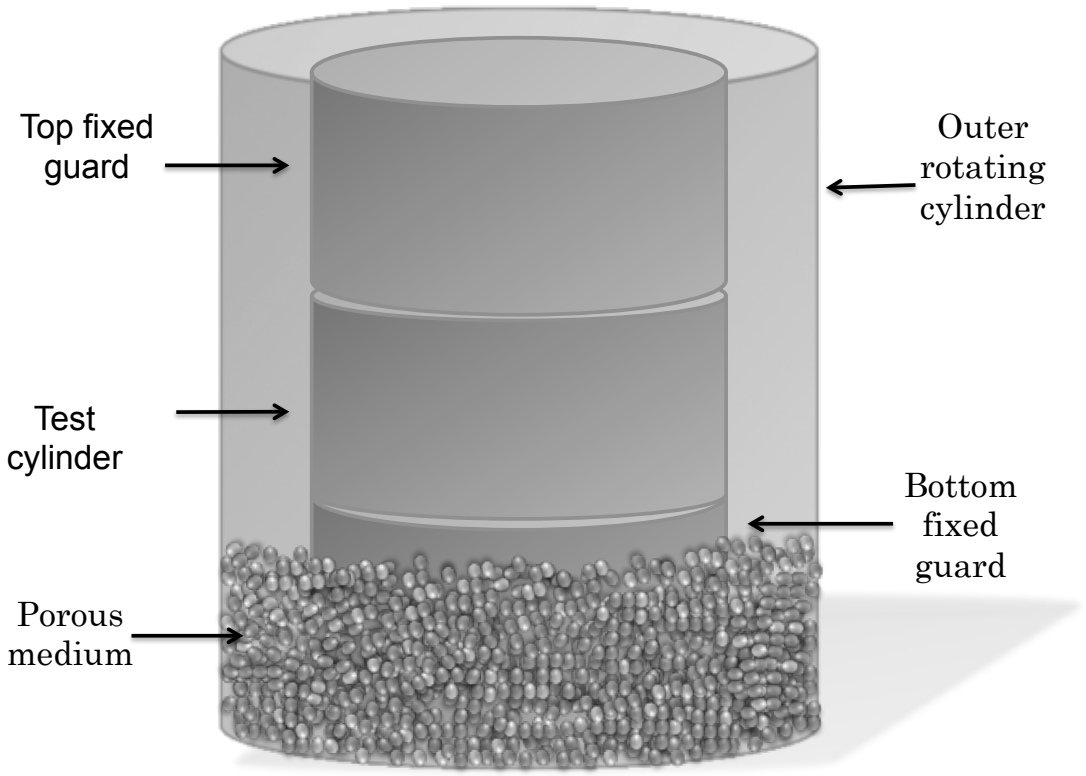

Figure 5.1: Scheme of the apparatus configuration for the experiments with flow over a porous medium.

are best fitted by a power law.

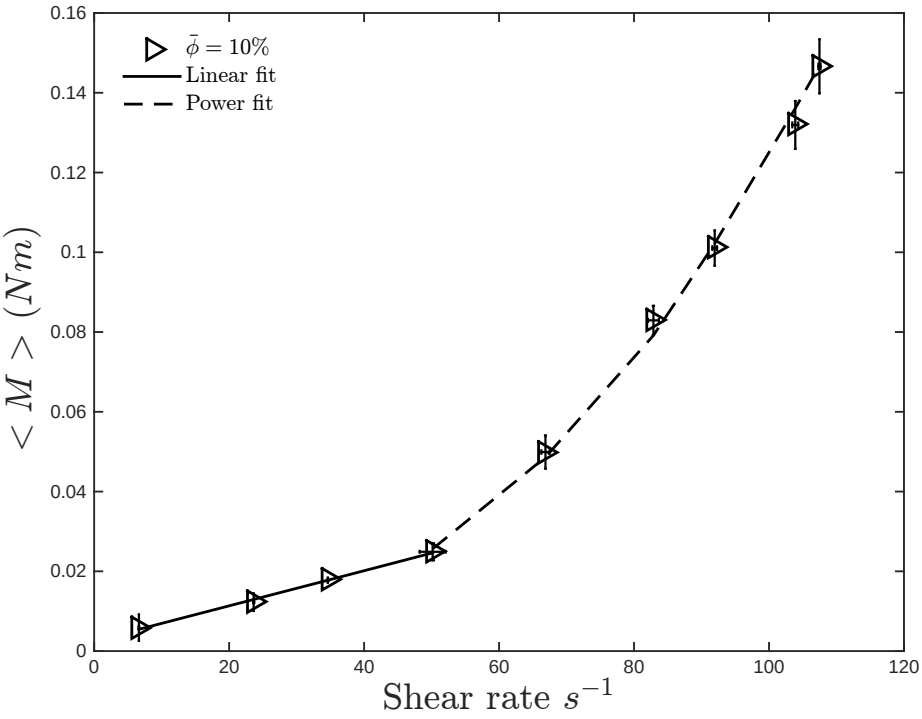

Figure 5.2: Measured torques as a function of the shear rate for flow over a porous medium for $\bar{\phi} = 10\%$ and $\rho_p/\rho = 1.05$. The error bars correspond to the combined uncertainty in the torque measurements.

Figure 5.3 presents the torque measurements for a loading fraction of 20%. Unlike the results for $\bar{\phi} = 10\%$, the torque measurements for shear rates lower than 60 s^{-1} do not seem to depend linearly on the shear rate. For shear rates higher than 60 s^{-1}, a sudden drop in the torque is observed. The torque decreases almost by half between $\dot{\gamma} = 36$ s^{-1} and $\dot{\gamma} = 68$ s^{-1}. Such decrease in the torque is not observed for $\bar{\phi} = 10\%$, nor it is observed for the previous experiments with no glass beads at the bottom. After the torque drops, it starts increasing with the shear rate and it exhibits a linear dependance. Different from what is observed for the experiments with no glass beads, the minimum torque measured for this loading fraction does not correspond to the lowest shear rates. The variation in the torque with the shear rate can be attributed to the presence of the porous medium and depends on the expansion of the polystyrene particles with shear rate. The drop in torque might be caused by the complete fluidization of the settling particles. An analysis of the resuspension of particles is presented in the following chapter.

Figure 5.4 shows the torque measurements for a $\bar{\phi} = 30\%$. For $\dot{\gamma} < 40$ s^{-1}, the torque increases with the shear rate and for shear rates between 40 and 50 s^{-1}, the torque remains constant. For shear rates higher than 50 s^{-1}, the torque starts decreasing until it increases again for shear rates higher than 90 s^{-1}. There is no sudden drop on the torque measurements for this loading fraction.

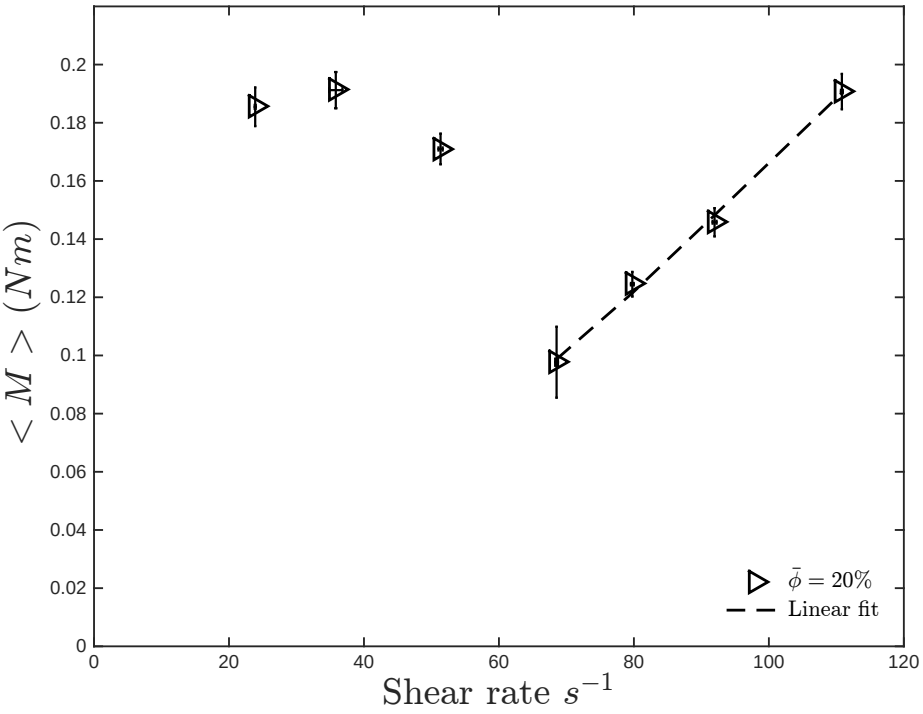

Figure 5.3: Measured torques as a function of the shear rate for flow over a porous medium for $\bar{\phi} = 20\%$ and $\rho_p/\rho = 1.05$. The error bars correspond to the combined uncertainty in the torque measurements.

However, the torque does decrease and similarly to what is found for a loading fraction of 20 %, the lowest torque measured does not correspond to the lowest shear rate.

A similar behavior is observed for higher loading fractions of 40 and 50 %, as shown in Figure 5.5. For low shear rates, the torque increases in a linear way. For shear rates higher than 60 s^{-1}, the torque dependance starts shifting. The torque starts to decrease for shear rates higher than 70 s^{-1}. For a loading fraction of 40 % and for shear rates higher than 100, the torque starts to increase again, while for $\bar{\phi} = 50\%$ the increase on torque starts at a lower shear rate of 91 s^{-1}. The decrease in the torque measured for a loading fraction of 50% is less pronounced than for lower loading fractions. For this loading fraction in particular, the minimum torque measured corresponds to the second lowest shear rates, while for the case of $\bar{\phi} = 40\%$, the lowest torque measured does not correspond to the lowest shear rate. As pointed out previously, this behavior is observed for the other loading fractions. If the decrease in torque is governed by the expansion of the particles, then for a high loading fraction this drop in the torque is less pronounced, since there is less space available for the particles to expand. Further discussion on the expansion of particles is presented in Chapter 6

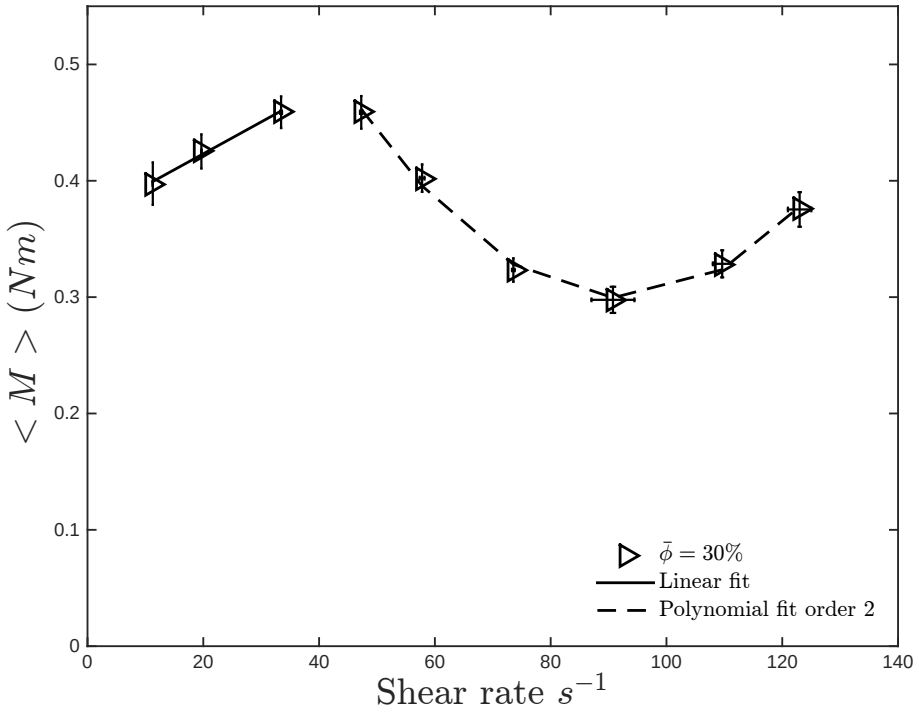

Figure 5.4: Measured torques as a function of the shear rate for flow over a porous medium for $\bar{\phi} = 30\%$ and $\rho_p/\rho = 1.05$. The error bars correspond to the combined uncertainty in the torque measurements.

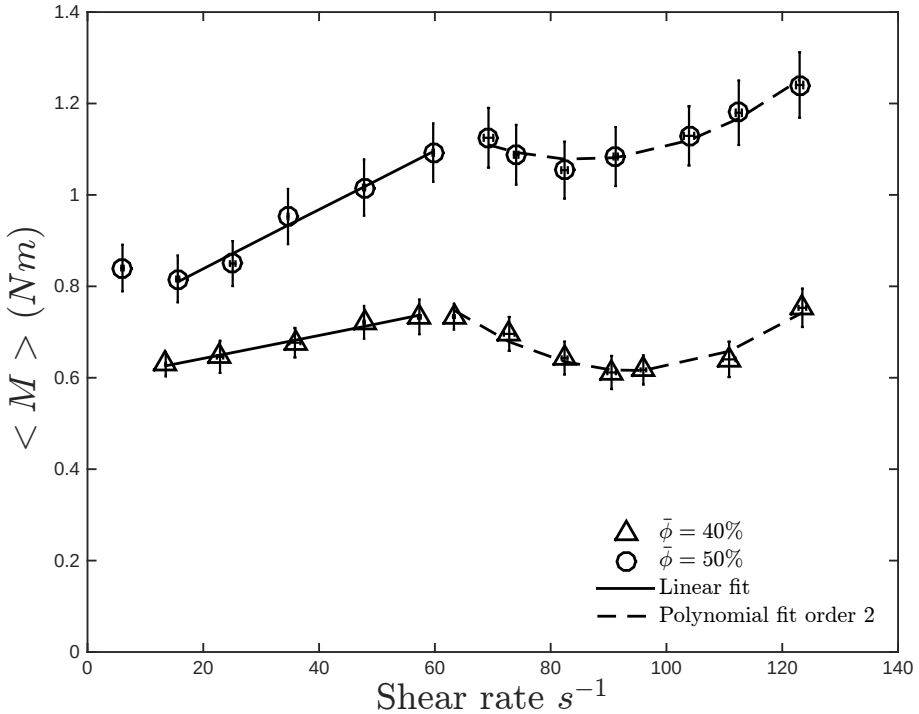

Figure 5.5: Measured torques as a function of the shear rate for flow over a porous medium for $\bar{\phi} = 40$ and 50% and $\rho_p/\rho = 1.05$. The error bars correspond to the combined uncertainty in the torque measurements.

Hysteresis

To study if there is a dependance on the shearing history of the mixture, torque measurements were made from high to low shear rates. These measurements were made right after the measurements from low to high shear rates were taken. Figure 5.6 shows the torque as a function of the shear rate for $\bar{\phi} = 10\%$, for both cases: from low to high and from high to low shear rates. For shear rates higher than 60 s^{-1}, the torque for both cases coincides. For lower shear rates, the torques corresponding to decreasing shear rates are higher.

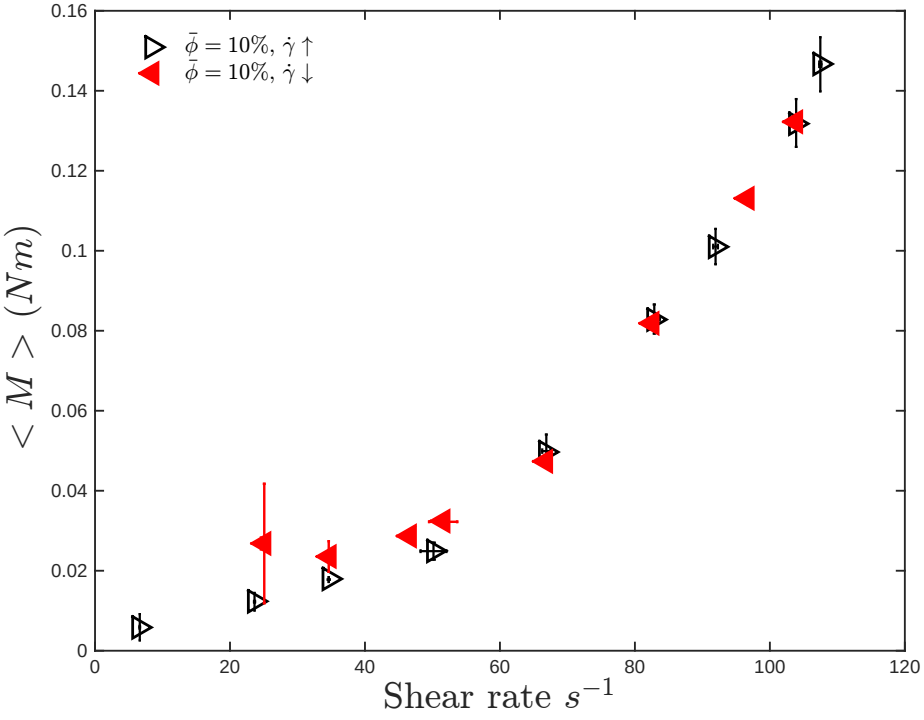

Figure 5.6: Measured torques for $\uparrow \dot{\gamma}$ and $\downarrow \dot{\gamma}$ for flow of settling particles over a porous medium with $\bar{\phi} = 10\%$ and $\rho_p/\rho = 1.05$. The error bars correspond to the combined uncertainty in the torque measurements.

For a loading fraction of 20%, the presence of hysteresis seems to be less pronounced, as shown in Figure 5.7. However, for low shear rates the torque measurements for the case with decreasing shear rate are slightly higher than the torque measurements with increasing shear rate.

Similarly, the hysteresis present for a loading fraction of 30% occurs for shear rates lower than 60 s^{-1}. But unlike $\bar{\phi} = 10$ and $\bar{\phi} = 20$, the torques measured for decreasing shear rates are lower than the ones measured for increasing shear rates, as shown in Figure 5.8. In the following section, it is shown that the apparent hysteresis found for $\bar{\phi} = 30\%$ is due to a change in the suspending liquid temperature.

As shown in Figure 5.9 for higher loading fractions of 40 and 50% the torque measurements for increasing and decreasing shear rate seem to match for all the shear rates tested.

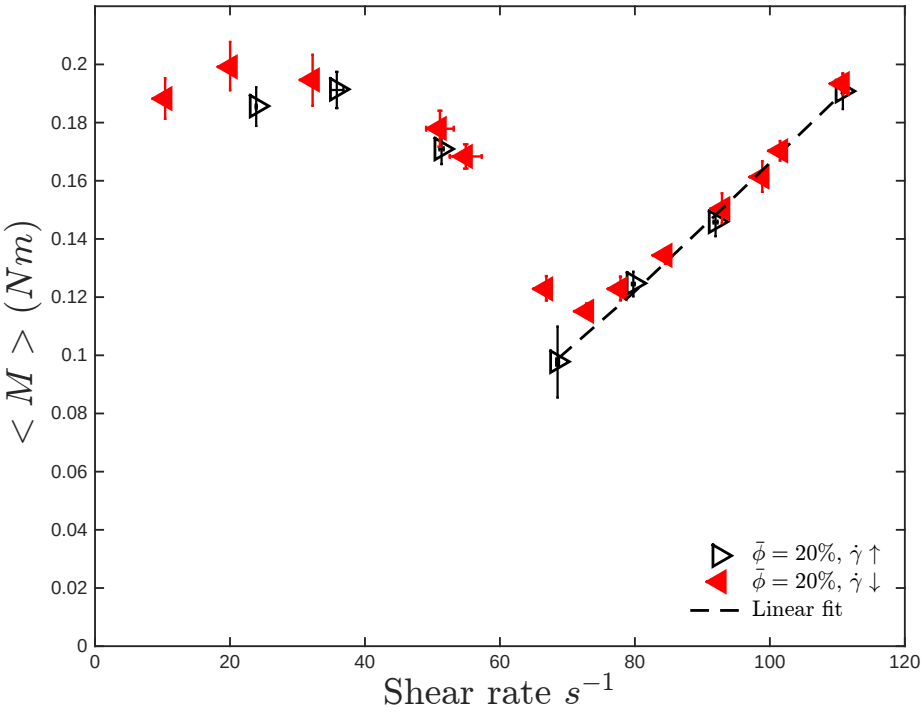

Figure 5.7: Measured torques for $\uparrow \dot{\gamma}$ and $\downarrow \dot{\gamma}$ for flow of settling particles over a porous medium with $\bar{\phi} = 20\%$ and $\rho_p/\rho = 1.05$. The error bars correspond to the combined uncertainty in the torque measurements.

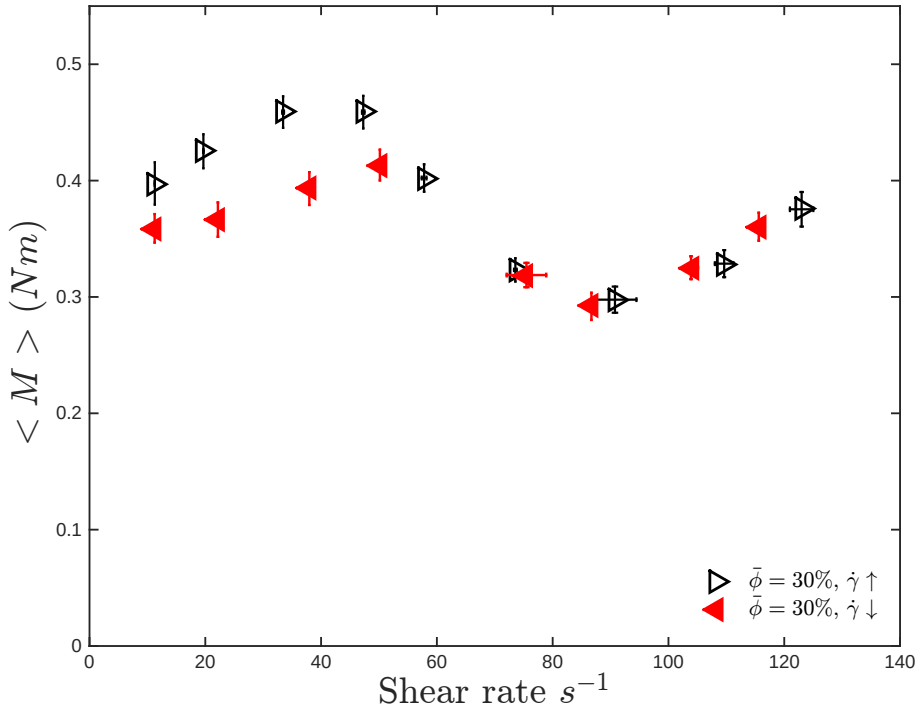

Figure 5.8: Measured torques for $\uparrow \dot{\gamma}$ and $\downarrow \dot{\gamma}$ for flow of settling particles over a porous medium with $\bar{\phi} = 30\%$ and $\rho_p/\rho = 1.05$. The error bars correspond to the combined uncertainty in the torque measurements.

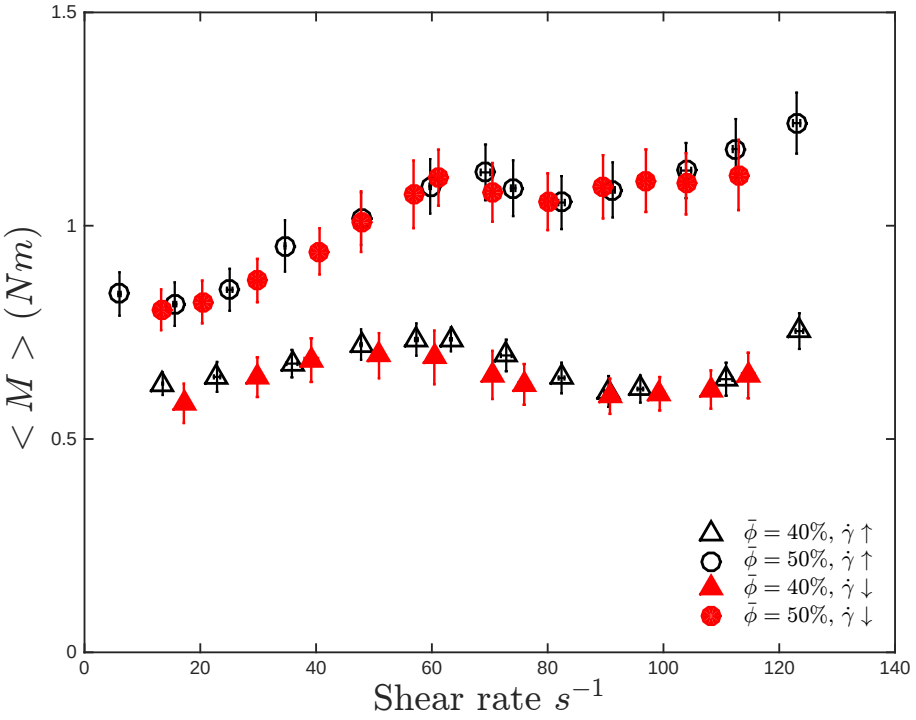

Figure 5.9: Measured torques for $\uparrow \dot{\gamma}$ and $\downarrow \dot{\gamma}$ for flow of settling particles over a porous medium with $\bar{\phi} = 40$ and 50% and $\rho_p/\rho = 1.05$. The error bars correspond to the combined uncertainty in the torque measurements.

5.4 Normalized torque for polystyrene particles over a porous medium with $\rho_p/\rho = 1.05$

Figure 5.10 shows the normalized torques for a loading fraction of 10%. Considering the case where the torque measurements were taken for increasing shear rates, the normalized torques are fairly constant for Stokes number between 25 and 80. The ratio of torques then increases with the Stokes number. A similar behavior is observed for the normalized torques measured with decreasing shear rates. For Stokes number lower than 100, the normalized torques seem to have a dependance on the shearing history of the mixture. The range of Stokes number at which the ratio of torques drops and remains constant also depends on the shearing history of the mixture.

Figure 5.11 presents the normalized torques for a loading fraction of 20%. The ratio of torques decreases with Stokes number for both increasing and decreasing shear rates. For the case with decreasing shear rate, the normalized torques are slightly higher. For Stokes number higher than 100, the normalized torques exhibit a fairly constant behavior and no hysteresis is observed in the torque measurements.

For a loading fraction of 30%, the normalized torques become constant for Stokes number higher than 120, as shown in Figure 5.12. For all the Stokes number tested, the ratio of torques seems to

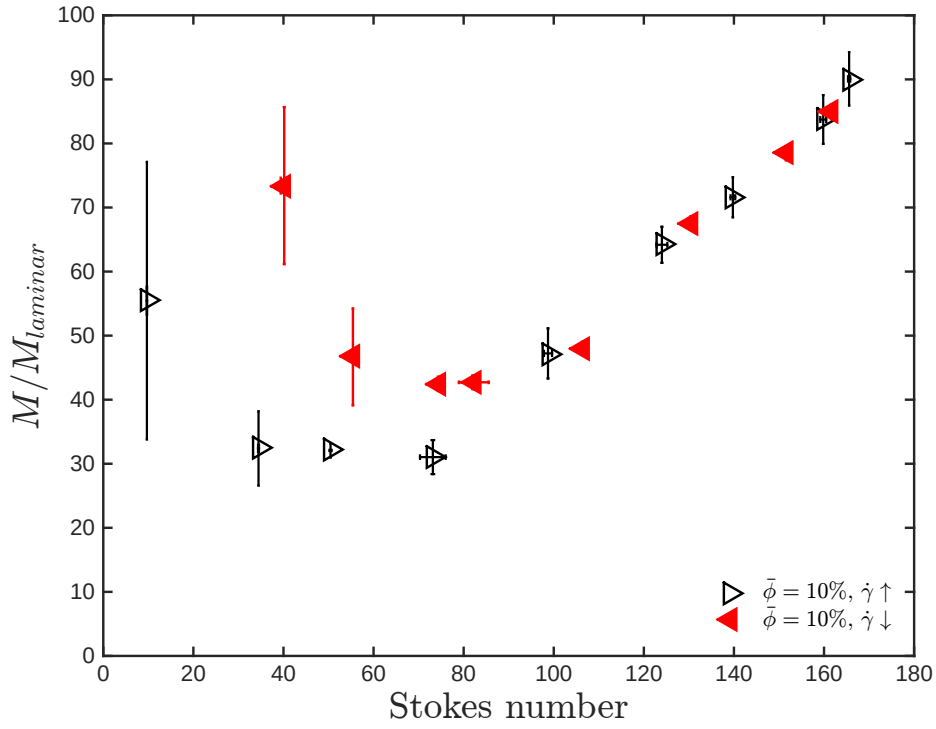

Figure 5.10: Normalized torques as a function of Stokes number for flows over a porous medium and $\phi = 10\%$ with $\rho_p/\rho = 1.05$. The error bars correspond to the combined uncertainty in the torque measurements normalized by the corresponding $M_{laminar}$.

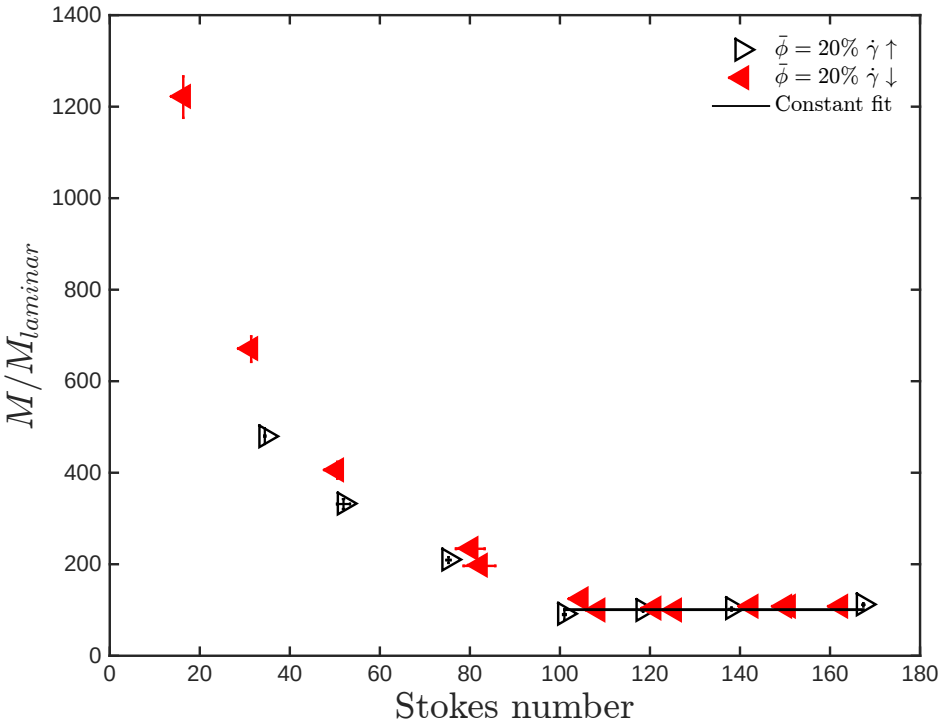

Figure 5.11: Normalized torques as a function of Stokes number for flows over a porous medium and $\phi = 20\%$ with $\rho_p/\rho = 1.05$. The error bars correspond to the combined uncertainty in the torque measurements normalized by the corresponding $M_{laminar}$.

show no hysteresis. This is different from what was observed in the previous section in Figure 5.4, where the measured torques show hysteresis. Hysteresis is not observed in Figure 5.12 because by normalizing the torque, the difference in the liquid viscosity due to an increase in temperature is considered.

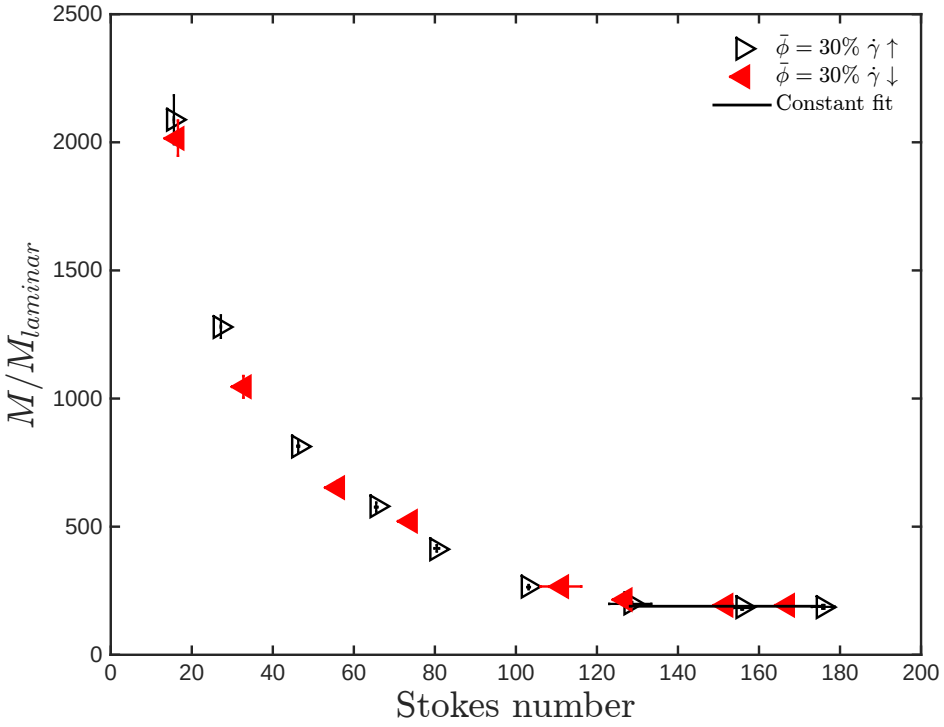

Figure 5.12: Normalized torques as a function of Stokes number for flows over a porous medium and $\phi = 30\%$ with $\rho_p/\rho = 1.05$. The error bars correspond to the combined uncertainty in the torque measurements normalized by the corresponding $M_{laminar}$.

Figure 5.13 shows the normalized torques for a loading fraction of 40 %. The ratio of torques corresponding to decreasing shear rates is slightly higher than for the case with increasing shear rates for Stokes numbers lower than 100. For Stokes number higher than 150, the normalized torques appear to be constant.

Figure 5.14 shows the normalized torques for the highest loading fraction tested for this type of experiments $\bar{\phi} = 50\%$. There seems to be no hysteresis for the whole range of Stokes numbers tested. The normalized torques decrease with Stokes number but unlike the lower loading fractions it did not become constant. This is better observed in a semi-log plot. Figure 5.15 shows the normalized torques for all the loading fractions tested. For $\bar{\phi} = 50\%$, the ratio of torques at the highest Stokes numbers suggests that $M/M_{laminar}$ may reach a constant.

As shown in Figure 5.15, for Stokes number lower than 100, the normalized torques decrease with Stokes number for all the loading fraction tested. For loading fractions higher than 10%, the normalized torques continue to decrease until they become constant, with the exception of $\bar{\phi} = 50\%$,

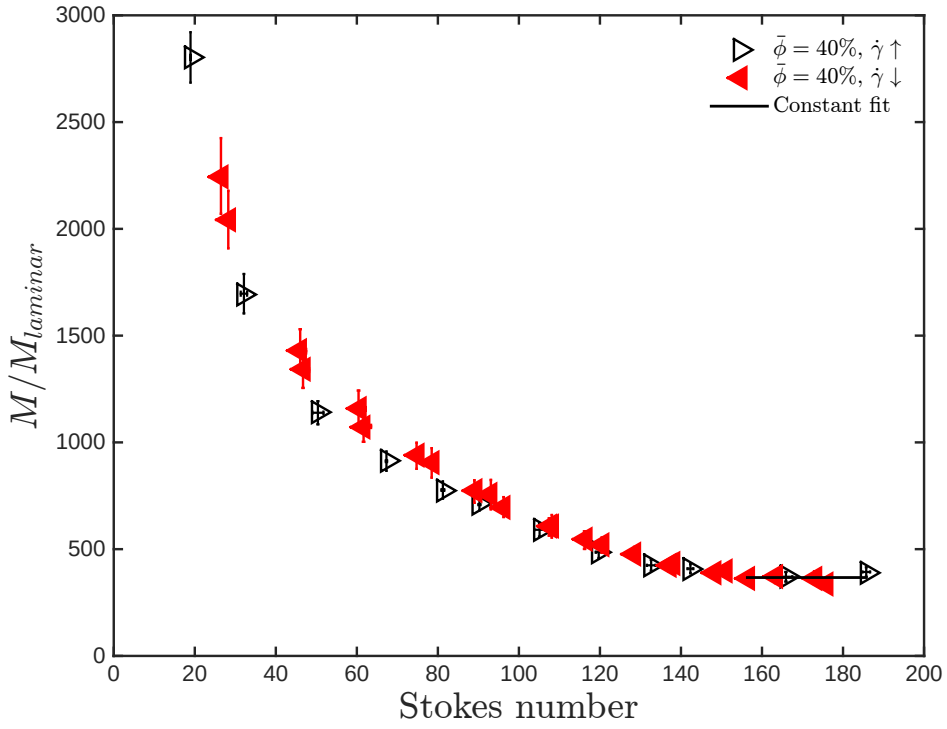

Figure 5.13: Normalized torques as a function of Stokes number for flows over a porous medium and $\phi = 40\%$ with $\rho_p/\rho = 1.05$. The error bars correspond to the combined uncertainty in the torque measurements normalized by the corresponding $M_{laminar}$.

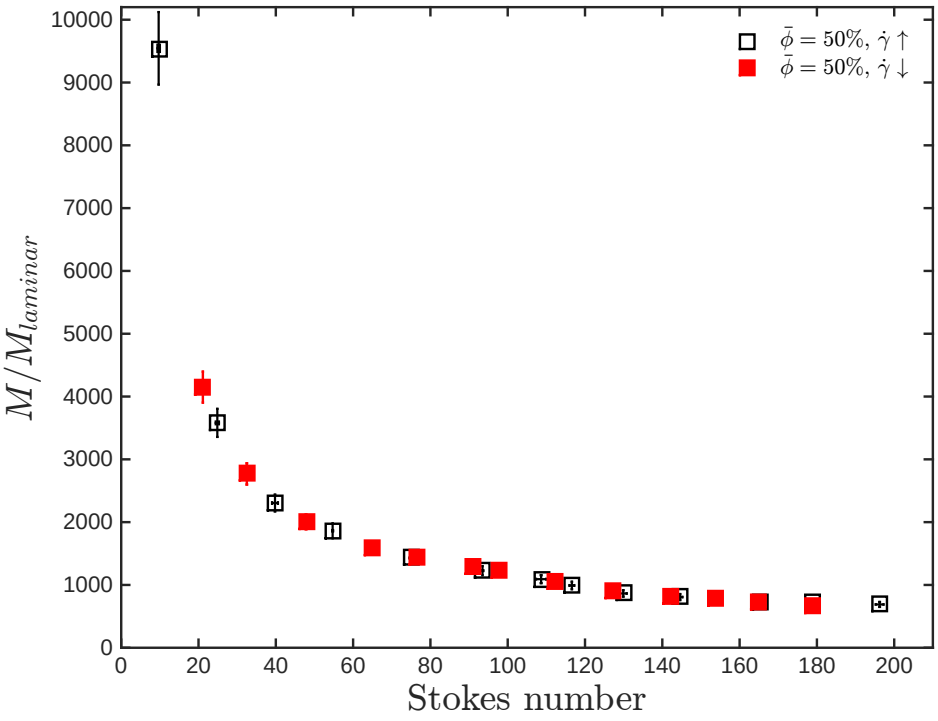

Figure 5.14: Normalized torques as a function of Stokes number for flows over a porous medium and $\phi = 50\%$ with $\rho_p/\rho = 1.05$. The error bars correspond to the combined uncertainty in the torque measurements normalized by the corresponding $M_{laminar}$.

where the normalized torque does not reach a plateau. For $\bar{\phi} = 10\%$, the normalized torques start increasing for $St > 80$. For this particular loading fraction, the maximum value for the normalized torque occurs at the lowest and the highest Stokes number.

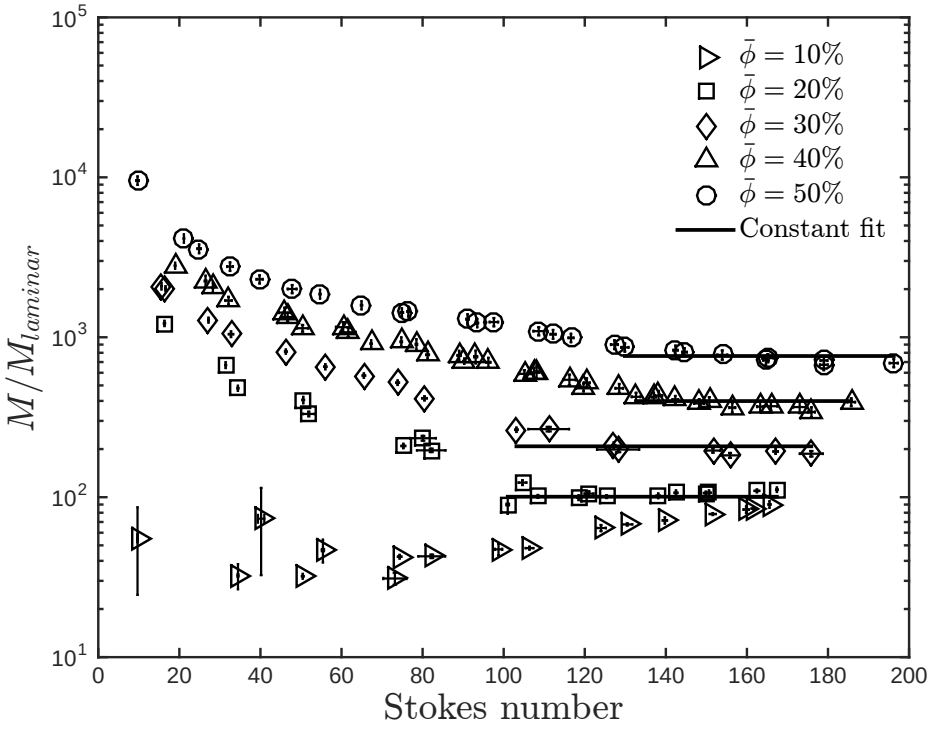

Figure 5.15: Normalized torques as a function of Stokes number for flows over a porous medium for all $\bar{\phi}$ tested with $\rho_p/\rho = 1.05$. The error bars correspond to the combined uncertainty in the torque measurements normalized by the corresponding $M_{laminar}$.

5.5 Summary

Results from experiments where the liquid-solid mixtures are sheared over a porous medium were presented. The torque measurements corresponding to shear rates lower than 60 s^{-1} increase with shear rate. For higher shear rates there is a change in the torque trend. For $\bar{\phi} = 10\%$, the torque dependance on shear rate became different: from linear to non linear (power law fit). For the rest of the loading fractions, the torque exhibits a drop where the torque decreases and then increases again with the shear rate. These marked changes in the dependance of the torque on shear rate are not observed in the experiments with no porous medium. The presence of hysteresis is studied and it is found that with the exception of $\bar{\phi} = 10\%$, once the torque is normalized there is no significant presence of hysteresis for all the loading fraction tested. In general, for Stokes number lower than 100, the normalized torques decrease with St. For a loading fraction of 10%, the normalized torques start to increase for $St > 80$. This increase is only observed for this particular loading fraction. For

the other loading fractions, the normalized torques decrease and for $\bar{\phi} < 50\%$ it becomes constant. The Stokes number at which the normalized torques reach a plateau increases with the loading fraction. For $\bar{\phi} = 10\%$, μ'/μ starts increasing for $St > 80$. For $\bar{\phi} = 20$, $\bar{\phi} = 30$, and $\bar{\phi} = 40$, μ'/μ becomes constant at $St > 120$, $St > 125$, and $St > 155$, respectively.